First-return maps as a unified renormalization scheme for dynamical systems

Itamar Procaccia, Stefan Thomae,* and Charles Tresser†
Chemical Physics Department, Weizmann Institute of Science, Rehovot, Israel 76100
(Received 30 June 1986)

We propose to look at first-return maps into a specified region of phase space as a basis for a unified renormalization scheme for dynamical systems. The choice of the region for first return is dictated by the symbolic dynamics (e.g., kneading sequence) of the relevant trajectories. The renormalization group can be formulated on the symbolic level, but once translated to maps it yields the said renormalization scheme. We show how the well-studied examples of the onset of chaos via period doubling and quasiperiodicity fit into this approach, and argue that these problems get in fact unified. The unification leads also to a generalization that allows us to study the onset of chaos in maps that belong to larger spaces of functions than those usually considered. In these maps we discover a host of new scenarios for the onset of chaos. These scenarios are physically relevant since the maps considered are reductions of simple flows. We present a theoretical analysis of some of these new scenarios, and report universal results. Finally we show that all the available renormalization groups can be found using symbolic manipulations only.

I. INTRODUCTION

The success of renormalization techniques in providing a theoretical framework for understanding the universality observed in dynamical systems at the onset of chaos,[1–5] has been quite remarkable. This success should be confronted, however, with the fact that up to now one had to come up with ingenious new approaches for every problem studied. One could not, for example, pick the techniques developed for period doubling[2,3] and apply them automatically to quasiperiodicity.[4,5] In some sense one still feels that there should be an underlying theory which might be more general and more powerful than the implementations seen so far.

In this paper we wish to describe an approach that goes in the direction of finding such a unified theory [6] The purpose is to find a method that could be applied in the very same way to a large number of different continuous flows in phase space which can be reduced to a one-dimensional map by Poincaré section. The basic idea is to use first-return maps (or "induced" map in the language of ergodic theory) as the foundation of a renormalization scheme. To understand this consider Fig. 1, for example, in which we see a limit cycle a that underwent a period doubling yielding a cycle b. The core of any renormalization is the attempt to do something that will transform the orbit b such as to resemble orbit a. The usual approach is to consider the Poincaré map on a transversal section through the orbit and then compare an iterate of this map, properly rescaled, with the original one. Alternatively, we suggest here to consider a first-return map into a subset J of the surface of section (see Fig. 1) on which the situation is similar to that seen on the complete section through the orbit a. Of course, in this example the two approaches coincide; we shall see in the following that in other instances one is led to return maps that are not simple iterates of the original mapping.

Clearly, the crucial questions are how to choose the region J (this, in fact, is also a crucial question in the usual approaches) and whether by repeating a procedure of this kind one generates a renormalization group. The answers to these questions in the context of dynamical systems that can be reduced to one-dimensional maps are the subject of this paper.

We shall show that the choice of the return region J for any given problem is dictated by the topology of the relevant orbits. This topology, represented as usual by symbolic dynamics, will allow the introduction of blocks of symbols, which are somewhat reminiscent of spin blocks in solid-state critical phenomena. The renaming of these blocks of symbols by a single symbol defines the renormalization group, but also determines the first-return

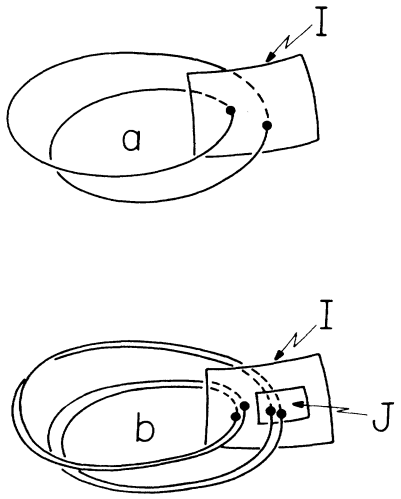

FIG. 1. First-return map for a limit cycle after period doubling. Reducing the surface of section from I to a subset J generates a first-return map of the double cycle b which is similar to the one of the original cycle a.

region J, as is shown below. This idea allows us to describe in a unified fashion the onset of chaos in continuous circle maps and one-hump maps of the interval as well as discontinuous maps featuring new scenarios for the onset of chaos.

It will be shown that one is led to the study of discontinuous maps. These maps appear as natural reductions of simple flows and exhibit a rich dynamical behavior including an infinity of different scenarios for the onset of chaos. It will be shown, however, that all these scenarios, which include also period doubling and quasiperiodicity, can be treated in a unified fashion with the ideas developed here.

It should be stressed from the start that we do not claim that the functional approach that has been developed for renormalizing dynamical systems should be discarded. Quite on the contrary, whenever we want to calculate universal numbers we turn to functional equations. It is our contention, however, that it becomes very clear what functional equation one should choose after the present approach has been dealt with. In all that follows the emphasis is on the formulation of the renormalization group rather than on questions like the existence of a fixed point, etc.

In Sec. II we introduce these ideas with the help of the familiar example of period doubling. Section III deals with circle maps. In Sec. IV we discuss the formal unification of circle maps and quadratic maps. An additional result of this unification is an enlargement of the space of functions that can be considered. We examine the new scenarios that are available in this space of functions and focus on a few of them. We present a detailed theory of period tripling. The functional equations are set and solved in ϵ expansion. Section V offers numerical tests of the theory of Sec. IV, with applications to the onset of chaos in maps and in flows. Section VI presents the tools needed for constructing a theory for any of the infinity of scenarios found in Sec. IV. In Sec. VII we present a global theory for the location of "good" renormalization groups, based on the encoding furnished by symbolic dynamics. The abundance of nongeometric "scaling" behavior will be stressed and linked to the existence of degenerate fixed points of the renormalization groups. A summary and discussion is given in Sec. VIII.

II. PERIOD DOUBLING AND RETURN-MAP RENORMALIZATION

Consider a map $f_\mu(x)$ of the interval I as shown in Fig. 2. Assume that as a function of the parameter μ this map exhibits a cascade of period doublings, and that the graph shown pertains to the parameter value $\mu=\mu_\infty$, at the point of accumulation of period doublings (i.e., this is the map f_{μ_∞}). We wish to define a first-return map into some interval $J\subset I$ with the aim of using it as a generator of a renormalization group. In order to do so we first remind ourselves of the kneading sequences of the 2^n-periodic superstable orbits.[7] For unimodal maps, where $f'(x_c)=0$, one defines $\chi(x)$ where x is any point in the interval by

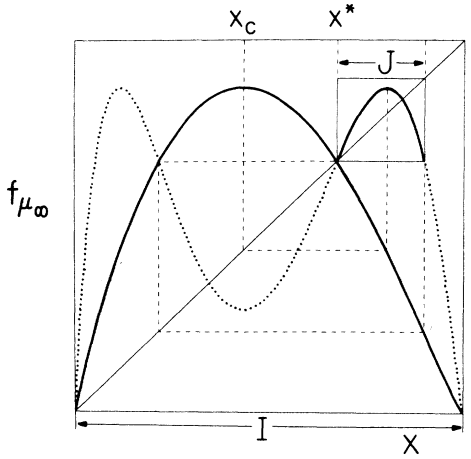

FIG. 2. First-return map for a one-hump map of the interval. The first-return map into the subinterval J is similar to the original one. The dashed lines indicate the relation between x_c, x^* and the features of the return map. Here the first-return map is the second iterate (dotted line) restricted to J. Note that its ascending branch corresponds to RR in the original map and its descending branch to RL.

$$\chi(x)=\begin{cases} L, & x<x_c \\ C, & x=x_c \\ R, & x>x_c \ . \end{cases} \tag{2.1}$$

Picking any initial point x_0 in I, the itinerary $I(x_0)$ of x_0 is defined by $[\chi(x_0),\chi(f(x_0)),\chi(f^2(x_0)),\ldots]$. The itinerary of $f(x_c)$ truncated after the first C is called the kneading sequence of the map. All cycles containing x_c are termed superstable. Thus a 2^0 superstable period is C. A 2^1 superstable periodic orbit is RC. As is well known, to obtain the kneading sequence of the 2^n superstable orbit we copy the kneading sequence of the superstable 2^{n-1} orbit twice, and change the C in the middle to R or L in an alternating fashion. Thus the kneading sequences of the next superstable 2^n-periodic orbits are

$$\begin{aligned} &R\underline{L}RC \text{ for } 2^2 , \\ &RLR\underline{R}RLRC \text{ for } 2^3 , \\ &RLRRRLR\underline{L}RLRRRLRC \text{ for } 2^4 , \\ &RLRRRLRLRLRRRLR\underline{R}RLRRRLRLRLRRRLRC \\ &\qquad\qquad\qquad\qquad\qquad\qquad\qquad\qquad\qquad\qquad \text{for } 2^5 , \end{aligned} \tag{2.2}$$

etc., where the underbar marks the alternating R or L that appears in this construction. Clearly, the head of the kneading sequence of the map f_{μ_∞} is represented by the sequences (2.2), truncated before the C. Considering now this kneading sequence we ask the following question: Is there a way to define blocks of symbols such that there are only two types of blocks (corresponding to the fact that there are two original symbols R and L) which can be then renamed R and L? As we shall see, this question will return in all the examples treated below. In a sense this question reminds one of the spin-block idea[8] in the context of renormalization groups of critical phenomena.

It is easy to see that in the case considered here picking two-symbol blocks leads to the generation of two types of blocks: RL and RR. (The block RC occurs only once, and only due to the finiteness of the sequence.) If we rename now the blocks according to $RL \to R$, $RR \to L$ ($RC \to C$), we see that the sequence of the 2^n cycle gets reduced to the sequence of the 2^{n-1} cycle. Clearly, the kneading sequence of f_{μ_∞} will remain invariant. We stress already here that invariance under the block-renaming procedure will not be required below. However, its existence is a minimal condition for the availability of a simple fixed-point theory (i.e., instead of, e.g., a periodic-point phenomenon).

We turn now to the meaning of the block-renaming procedure in terms of the first-return maps. A first-return map is a map of a subinterval $J \in I$ to itself, which is obtained by iterating the map with initial points x in J, and associating with each x the first point of its forward orbit which belongs to J. The reader recognizes that this is the map analog of the Poincaré first-return map for flows. The key idea now is that we shall interpret a block which appears in the block-renaming procedure as actual itinerary of the image of a point belonging to the interval J and the trajectory of which is truncated after it returns to the interval J for the first time. Every R will mean an iteration with a right branch (i.e., f_μ restricted to $x > x_c$), and an L with a left branch (i.e., f_μ restricted to $x < x_c$). Since our blocks in this case start with R, J has to lie to the right of x_c. It cannot be, however, the whole right interval, because points near the fixed point x^* would return after one R. Therefore, J must lie either to the right or to the left of x^*. Since no point between x_c and x^* has an itinerary $RL \ldots$, J must lie to the right of x^*. In order to return after at most two iterations to the right of x^* the initial point must lie to the left of the second preimage of x^* which is larger than x^*. This leads to a choice of J as shown in Fig. 2. One can check now that every point in this interval J returns after two iterations either RR or RL. The graph of the first-return map that we are after will appear therefore in the box $J \times J$ shown in Fig. 2. One should stress that this choice of the interval J is not unique. A smaller interval could do as well. There is in fact a range of J's between the minimal and maximal ones which yield return maps which are equivalent from the renormalization-group (RG) point of view. The somewhat nonsystematic way that J was chosen above could be replaced by an algorithm. We chose not to do it here since later we shall see that in a space of functions where period doubling gets unified with quasiperiodicity such an algorithm appears in a very natural and simple way.

This first-return map on J is, of course, nothing else but the second iterate of the map f_{μ_∞}, restricted to J. It has again right and left branches separated by the right preimage of x_c, which becomes the new C. Of course, this point separates J into two segments, the right one, leading to $RL \to R$, and the left one, which is responsible for $RR \to L$.

As an example of f_{μ_∞}, consider the quadratic map $\tilde{x} = (3.5699) \cdots x(1-x)$. The nonzero fixed point of this map is $x^* = 0.7198\ldots$. The right boundary of J is $0.9141\ldots$. The point $0.8315\ldots$, which is the right preimage of x_c, separates $RL \to R$ from $RR \to L$.

In order to repeat the procedure we can rescale J to size unity. The scaling factor here is $\beta^{(1)} = 5.1467\ldots$. The new map has the same kneading sequence as the first one, and the procedure can be iterated. The next J interval can be found easily, and its scaling ratio to the first J gives $\beta^{(2)} = 6.5864\ldots$. This scaling factor goes asymptotically to β, which is α^2 in the language of Ref. 3.

We recognize the following facts.

(i) The procedure obtained here is identical in results, if not in spirit, to the one perceived in Ref. 4.

(ii) The return maps in the smaller and smaller J intervals will converge to a universal function once rescaled properly. Notice that in this first-return box the universal function is not symmetric.

(iii) We can examine first-return maps into J' whose right edge is the fixed point x^* and whose left edge is the left preimage of x^*. This generates a scheme whose scaling numbers $\beta^{(n)}$ converge to α. This is the most usual renormalization considered in the literature. This scheme is obtained by dropping the first R symbol in the kneading sequences (2.2), and then considering the blocks LR and RR in the kneading sequences. By renaming $LR \to R$, $RR \to L$ we obtain the interval J' shown in Fig. 3. In this interval the resulting fixed-point map is even, in contrast to the skew one that one gets in the process in Fig. 2.

(iv) The two choices of J intervals discussed above lead to order preserving (positive scaling number α^2) and order reversing (negative α), respectively. This could be read directly from the block renaming. In the language of Ref.

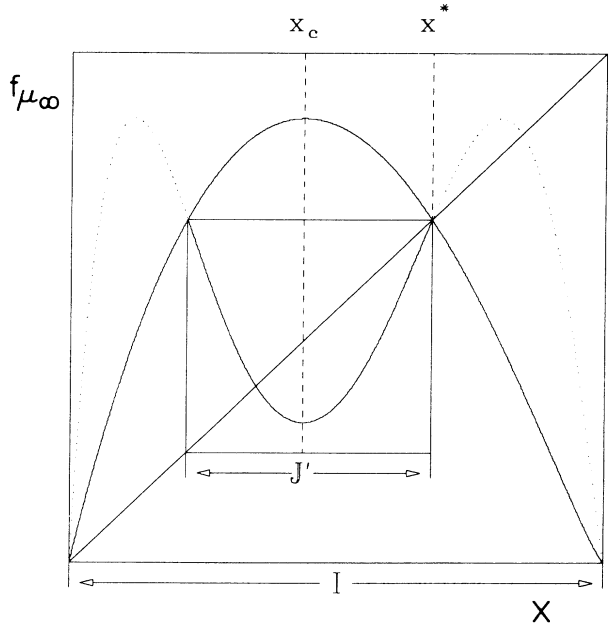

FIG. 3. Alternative choice of the return interval for one-hump maps. Iterating the return-map construction with this choice of the return interval leads asymptotically to a symmetric function even if the original map is not symmetric.

7, $RL > RR > LR$, $R > L$ for unimodal maps. [In general, "order" for symbolic sequences is defined by requiring that for $x > y$, $I(x) \geq I(z)$]. Therefore [$RL \to R$, $RR \to L$] is order preserving, whereas [$LR \to R$, $RR \to L$] is order reversing.

III. CIRCLE MAPS

In this section we consider subcritical and critical smooth circle maps $G(x)$. By "subcritical" we mean maps of the circle whose slope $G'(x)$ is positive everywhere. Critical maps have points where $G'(x)=0$, but are still monotonic. We begin by examining general properties of kneading sequences for such maps. Discontinuous maps of the circle will be considered in Sec. IV.

The easiest way to carry over the kneading techniques to circle maps is to represent the maps $G(x)$ as discontinuous maps $g(x)$ from the interval to itself. Denoting the point of discontinuity by x_c, we shall adopt the convention that $g(x_c)$ is $\lim_{x \to x_c} g(x)$. Thus we can define left and right branches as before as the restriction of $g(x)$ to $[0,x_c]$ and $(x_c,1]$, respectively. Note that this is slightly different from the usual definition using a reduction mod1. We remember that for continuous circle maps

$$g(0)=g(1)\ , \tag{3.1}$$

see Fig. 4.

We define an itinerary of a point x as before, and two kneading sequences K^+ and K^- as the itineraries of 1 and 0, respectively. Due to Eq. (3.1) K^+ and K^- are the same except for the first symbol. Hence, the use of two kneading sequences is not mandatory here; one can construct a consistent theory with only one. The reason that we define two kneading sequences is that it becomes essential in the sequel and is convenient here also. We can

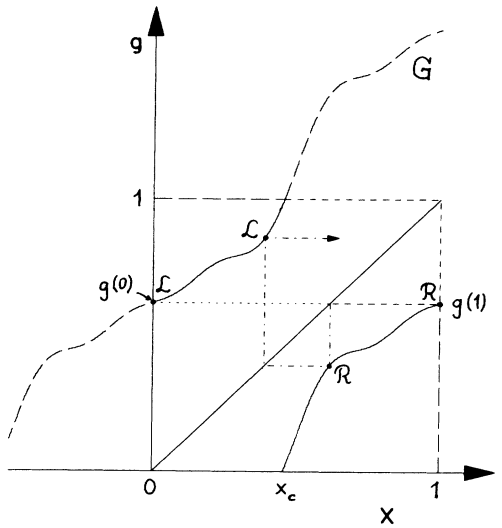

FIG. 4. Continuous circle maps. The reduction of the continuous map G (long dashes) leads to a discontinuous map of the interval [0,1]. The trajectories of 0 (dotted) and 1 (short dashes) meet after one iteration continuing on the same path (dash dotted). Hence the kneading sequences K^+ and K^- differ in the first symbol, only.

define the winding (or rotation) number w of a point as the limit of the ratio of R's to the total number of symbols in longer and longer truncations of its itinerary. As is well known, in the monotonic case this limit exists and does not depend on the initial point. We thus can refer to the winding number of the map. Of course, this definition of winding number is equivalent to the one adopted usually.[9]

The block structure of the kneading sequence[10] can be found for the following two cases: (i) $g(0)=x_c$ and (ii) $g(0) \neq x_c$. In case (i) $g(x)$ exchanges R and L in every iteration, and the kneading K^+ and K^- will be $RLRLRL\ldots$ and $LLRLRLR\ldots$, respectively. In case (ii) there will always be a branch whose domain is mapped completely into the domain of the other, see Fig. 5(a). Consequently, the kneading sequence K^+ can have the structure $R^{n_1}LR^{n_2}LR^{n_3}L$ for $w > \frac{1}{2}$, and K^- has the structure $L^{n_1}RL^{n_2}RL^{n_3}R$ for $w < \frac{1}{2}$. In the case $w = \frac{1}{2}$ one can have either $(K^-,K^+)=(L(RL)^\infty,(RL)^\infty)$ or $(K^-,K^+)=((LR)^\infty,R(LR)^\infty)$; we will also include the first (second) case when dealing with $w < \frac{1}{2}$ ($w > \frac{1}{2}$). Taking the case $w > \frac{1}{2}$, we notice that $g(0)$ iterates on the right branch a minimal number of times before coming back, and this is the minimal n_i in the kneading sequence. The point x_c iterates the maximal number of times, giving the maximal value of n_i. However, $g^2(x_c)=g(0)$ and therefore

$$\max\{n_i\}=\min\{n_i\}+1\ . \tag{3.2}$$

Thus the only values assumed by n_i are of the form n and $n+1$. A similar conclusion is obtained for the case $w < \frac{1}{2}$. The kneading sequences have therefore natural block structures with two blocks. These block structures will be preserved under different types of block renaming. In order to present these various possibilities without compromising transparency we do not split the discussion to the case $w < \frac{1}{2}$ and $w > \frac{1}{2}$, but only specify where one cuts the kneading sequence to produce blocks. One can either cut after each L, a procedure that we call an operator l,

$$l: \begin{cases} R^{m+1}L \to R \\ R^mL \to L\ , \end{cases} \tag{3.3}$$

where m can be zero, or after every R, yielding an operator r,

$$r: \begin{cases} L^{m+1}R \to L \\ L^mR \to R\ , \end{cases} \tag{3.4}$$

where again m can be zero. Notice that both l and r are order-preserving, since contrary to the one-hump maps [see remark (iv) of Sec. II] the natural ordering here is $R^{m+1}L > R^mL$, $L^mR > L^{m+1}R$, and $R > L$. The order-reversing case is discussed below.

The consequences of this block renaming for first-return maps will be drawn shortly. Before that, however, we discuss the transformation on the winding number that is implied.

Consider the operator l. For concreteness examine K^+ for $w > \frac{1}{2}$. The kneading sequence looks like

$$\overset{R^{n+1}L\ R^{n+1}L\ R^{n}L\ R^{n+1}L\ R^{n}L}{R \quad R \quad L \quad R \quad L \cdots}, \tag{3.5}$$

where the block renaming has been performed. Suppose also that $w=p/q$. What is the new $\tilde{w}=\tilde{p}/\tilde{q}$?

We recognize that $w=p/q$ means that within a period of the symbolic sequence we have a total of q symbols, p of which are R's. We thus have $q-p$ L's. Since each L defines a block,

$$\tilde{q}=q-p\ . \tag{3.6}$$

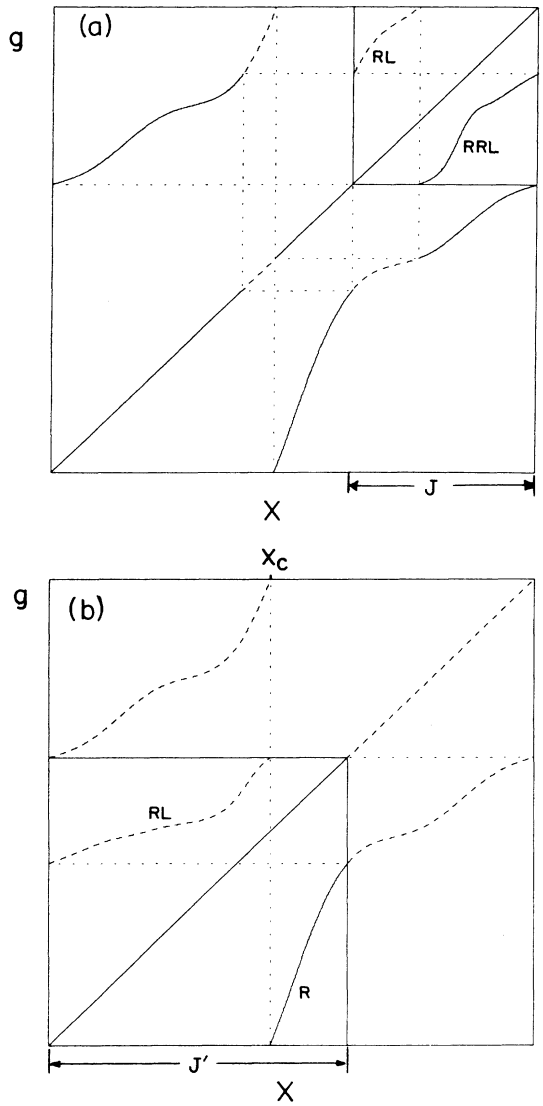

FIG. 5. First-return maps for a circle map with $w>\frac{1}{2}$. The domain of the left branch is mapped completely into the domain of the right one. Therefore itineraries cannot contain two or more consecutive L's. (a) l operator: Choosing J as intersection of the range of the left branch with the domain of the right one leads to a first-return map with branches corresponding to RL (second iterate) and RRL (third iterate). (b) r operator: Applying the r operator onto the same map leads to the return interval J' as shown. Hence the branches of the return map are parts of the second and first iterate.

Now $\tilde{p}$ is the number of R's in the new sequence, which is the number of times that $n_i=n+1$. To get this number we realize that $[p/(q-p)]$ (where [ ] denotes the integer part) is the number of R's that can be distributed evenly among the blocks. Thus the number of times $n_i=n+1$ is

$$\tilde{p}=p-(q-p)[p/(q-p)]\ . \tag{3.7}$$

Accordingly,

$$\tilde{p}/\tilde{q}=\tilde{p}/(q-p)=p/(q-p)-[p/(q-p)]\ . \tag{3.8}$$

More generally,

$$\tilde{w}=w/(1-w)-[w/(1-w)]\ . \tag{3.9}$$

In fact, the hypothesis $w>\frac{1}{2}$ is not needed for deriving Eq. (3.9), and it is the general consequence of the operator l. [If $w<\frac{1}{2}$, l leads to $\tilde{w}=w/(1-w)$]. Similarly, treating the operator r one gets the general formula

$$\tilde{w}=2-1/w+[(1-w)/w]\ , \tag{3.10}$$

which reduces to $\tilde{w}=2-1/w$ for $w>\frac{1}{2}$. Notice that the golden mean $w_G=(\sqrt{5}-1)/2$ is one of the fixed points of (3.9) whereas $1-w_g$ is one of the fixed points of (3.10). We remark that the transformations (3.9) and (3.10) are different from the Gauss map $\tilde{w}=1/w-[1/w]$ which corresponds to a shift of the coefficients in the continued fraction representation and played a central role in the formulations of the RG of circle maps.[5] In the language developed here the Gauss map is obtained from the order-reversing operator s,

$$s:\begin{cases} L^{m+1}R\to R \\ L^{m}R\to L\ . \end{cases} \tag{3.11}$$

At this point we can return to the issue of return maps. Choosing the l operator and considering the resulting blocks as actual itineraries that start with R (i.e., the first iteration is on the right branch) and return after one L, one finds J as the intersection of the domain of the right branch with the range of the left branch. We thus want to consider first-return maps into the interval J shown in Fig. 5(a). Similarly the operator r leads to J' as shown in Fig. 5(b). Notice that here the choice of return intervals is clearly determined once the blocks are specified.

As a simple demonstration of these considerations we examine circle maps with a golden-mean winding number. The golden mean w_G is the limit of F_n/F_{n+1} where F_n are Fibonacci numbers, defined by $F_{n+1}=F_n+F_{n-1}$, $F_0=F_1=1\ldots$, F_n/F_{n+1} and F_{n+1}/F_{n+2} are Farey neighbors; p/q and p'/q' are referred to as Farey neighbors if

$$|pq'-p'q|=1\ . \tag{3.12}$$

If the kneading sequence of a map with $w=p/q$ is A^∞ where A is a sequence of R's and L's, and for $w=p'/q'$ the kneading sequence is B^∞, then one can prove that the map with $w=(p+p')/(q+q')$ has kneading sequence $(AB)^\infty$ if $p/q>p'/q'$ and p/q and p'/q' are Farey neighbors. Accordingly, the kneading sequences K^+ for $w=1$, $\frac{1}{2}$, $\frac{2}{3}$, $\frac{3}{5}$, $\frac{5}{8}$, $\frac{8}{13}$, $\frac{13}{21}$, etc., are

$$
\begin{array}{ll}
1 & R \\
\frac{1}{2} & RL \\
\frac{2}{3} & R\ RL \\
\frac{3}{5} & RRL\ RL \\
\frac{5}{8} & RRL\ RRLRL \\
\frac{8}{13} & RRLRRLRL\ RRLRL \\
\frac{13}{21} & RRLRRLRL\ RRLRRLRLRRLRL
\end{array}
\tag{3.13}
$$

Using the l operator we find the blocks RRL and RL which are renamed $RRL \to R$, $RL \to L$. This leaves the kneading sequence K^+ for $w = w_G$ invariant. In terms of maps we can denote by g_R and g_L the map g restricted to R and L, respectively, and deduce the functional equations

$$
\begin{aligned}
\tilde{g}_R(x) &= \alpha g_L \circ g_R \circ g_r(x/\alpha) , \\
\tilde{g}_L(x) &= \alpha g_L \circ g_R(x/\alpha) ,
\end{aligned}
\tag{3.14}
$$

where α is the positive rescaling ratio of J to the interval.

The usual functional equation is obtained from the order-reversing operator s [Eq. (3.11)], with $m=0$, which turns K^- for the golden mean, i.e., $LRLRRLRLRRLRRLRLRRLRL \ldots$, into the corresponding K^+. This operator yields blocks LR, R, which are renamed $LR \to R$, $R \to L$ resulting in functional equations

$$\tilde{g}_R(x) = \alpha g_R \circ g_L(x/\alpha) , \tag{3.15a}$$

$$\tilde{g}_L(x) = \alpha g_R(x/\alpha) , \tag{3.15b}$$

with a negative α. At the fixed point we write $g_L(x/\alpha) = \alpha g_r(x/\alpha^2)$ which substituted in Eq. (3.15a) gives

$$g_R(x) = \alpha g_R \alpha g_R(x/\alpha^2) . \tag{3.16}$$

This is the functional equation considered and solved in Refs. 4 and 5.

IV. UNIFYING ONE-HUMP MAPS WITH CIRCLE MAPS

The discussion of Secs. II and III shows that the formulation of the renormalization group for unimodal and circle maps is actually unified by the concept of return map; the unification is realized by understanding the encoding furnished by symbolic dynamics.[11] In this section we pursue the unification further, and show how it can be achieved also on the level of operators acting on maps rather than on sequences.

In the process of unification we shall enlarge the space of functions under discussion. In this space of functions there are new scenarios for the onset of chaos. It is worthwhile to study these scenarios because the maps living in the larger space of functions appear as natural reductions of certain flows. Thus analyzing these new scenarios will allow us to offer new predictions for physical systems.

A. General remarks

Unimodal maps of an interval and circle maps look very different and there is no way to deform one case to the other. However, the following three remarks indicate that this difference can be surmounted. (i) The RG theory for one-hump maps can be done in the interval J' of Fig. 3, which leads to even fixed-point maps. Thus one loses nothing by restricting oneself to even maps.[12] Let then $f:[-\frac{1}{2},\frac{1}{2}] \to [-\frac{1}{2},\frac{1}{2}]$ be an even unimodal map with $f(0)=\frac{1}{2}$. Construct now the associated map $\tilde{u}(x):[-\frac{1}{2},\frac{1}{2}] \to [-\frac{1}{2},\frac{1}{2}]$ which is defined by

$$\tilde{u}(x) = \begin{cases} f(x), & x < 0 \\ -f(x), & x > 0 , \end{cases} \tag{4.1}$$

see Fig. 6. We shall see below that the knowledge of the dynamics of $\tilde{u}$ yields the dynamics of f uniquely (and vice versa).

(ii) We observe the fact that the renormalization-group transformation does not preserve the smoothness of the circle map. Since a transformed map has two branches which can be different iterates of the original one, the derivatives are in general discontinuous at the ends of these branches. Thus a natural space of functions which allows application of the renormalization group is the space of piecewise increasing smooth maps g from the interval $[-\frac{1}{2},\frac{1}{2}]$ to itself, with a single discontinuity at 0 and with the boundary conditions

$$g(0) = \tfrac{1}{2}, \quad \lim_{x \searrow 0} g(x) = -\tfrac{1}{2} , \tag{4.2a}$$

$$g(-\tfrac{1}{2}) = g(\tfrac{1}{2}) . \tag{4.2b}$$

(iii) If one suppresses the antisymmetry condition

$$\tilde{u}(-x) = -\tilde{u}(x) \tag{4.3}$$

for maps of remark (i) or the second boundary condition (4.2b) for the maps of remark (ii), one ends up with the same space $\overline{U}$ of piecewise increasing maps from $[-\frac{1}{2},\frac{1}{2}]$ to itself. A typical example of a two-parameter family of maps in the space of functions $\overline{U}$ is $\bar{u}_{\mu,\nu}(x)$,

$$\bar{u}_{\mu,\nu}(x) = \begin{cases} \frac{1}{2} - \mu x^2, & -\frac{1}{2} \le x \le 0 \\ -\frac{1}{2} + \nu x^2, & 0 < x \le \frac{1}{2} \end{cases} \tag{4.4}$$

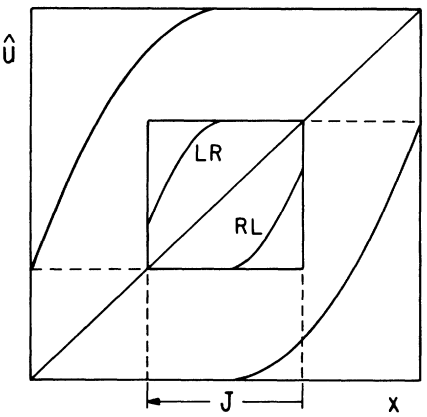

FIG. 6. The first-return map for antisymmetric maps $\tilde{u}$ with $RL \to R$, $LR \to L$.

with $\mu,\nu\in[0,4]$. We notice that the choice $\mu=\nu$ leads to maps of the type of $\tilde{u}$, Eq. (4.1), which are equivalent to one-hump maps, whereas $\mu=4-\nu$ leads to continuous circle maps. More generally the space $\bar{U}$ has two codimension-1 subspaces, one for continuous circle maps and one for maps which are equivalent to one-hump maps. It turns out that the space $\bar{U}$ does not contain all the available fixed points of renormalization groups that occur in it. It is necessary to enlarge $\bar{U}$ to the space U defined by dropping the condition that the discontinuity of the graph has to be in the center of the interval ($x_c=0$). The codimension-1 subspaces of U corresponding to one-hump maps and continuous circle maps will be called "first diagonal" and "second-diagonal," respectively, in analogy to their role in $\bar{U}$. In Sec. IV C we examine the scenarios for the onset of chaos for functions in the space U. As a preparation we first discuss kneading sequences. In all that follows we will consider maps in U as maps of the circle or of the interval according to the problem at hand.

B. Kneading sequences for maps in U

The essential difference between the kneading sequences of continuous circle maps and other maps in U is that for the former K^+ and K^- differ in only one symbol, whereas for the latter K^+ and K^- can be totally different. For antisymmetric maps of the type of Eq. (4.1) the situation is simple. The sequences K^+ and K^- go to one another simply by replacing R and L and vice versa. We can find the kneading sequences of these maps by realizing that there is a simple relation between the dynamics of $\tilde{u}(x)$ and $f(x)$. This relation is[13]

$$\tilde{u}^n(x_0)=\mathrm{sgn}[(df^n/dx)_{x_0}]f^n(x_0)\ . \tag{4.5}$$

This relation allows us to go from an itinerary I_f of a point under the map f to $I_{\tilde{u}}$ of the same point under $\tilde{u}$, and vice versa. Notice that both for f and $\tilde{u}$ the sign of a point indicates in the same way where it is on R or on L. Consequently, if $f^n(x)$ and $\tilde{u}^n(x)$ have the same sign, it means that the nth symbol in the itineraries $I_f(x)$ and $I_{\tilde{u}}(x)$ are the same. However, from Eq. (4.1) we see that if the sign of $\tilde{u}^n(x)$ and $f^n(x)$ coincide, then $d(f^n)/dx>0$. Since f has negative derivatives on R only, we conclude using the chain rule that among the first n symbols of the itinerary I_f there was an even number of R's. Similarly, the nth symbol of I_f and $I_{\tilde{u}}$ will differ if the number of preceding R's in I_f is odd. Consequently, we can give the following rules for transforming I_f to $I_{\tilde{u}}$ and vice versa.

Having I_f, we copy its symbols, switching $R\leftrightarrow L$ whenever the number of preceding R's in I_f is odd, and leaving the symbol as it is if the number of preceding R's in I_f is even. Having $I_{\tilde{u}}$, we copy the symbols switching $R\leftrightarrow L$ if the number of R's already existing in the resulting I_f is odd, and leaving the symbol unchanged if the number of generated R's is even. In all cases a C remains invariant.

Example:

$$\begin{aligned} &RLRRLLRRRLLLC \quad \text{for } I_f\ , \\ &RRLRRRLRLLLLC \quad \text{for } I_{\tilde{u}}\ . \end{aligned} \tag{4.6}$$

C. Unifying known RG's on the level of maps

In U we have a codimension-1 subspace of continuous (critical) circle maps. The discussion of Sec. III is immediately adoptable to maps of this subspace and there is no need for further discussion. On the other hand the codimension-1 subspace of maps of the type of $\tilde{u}(x)$ needs further analysis. Transforming the last kneading sequence in (2.2) according to the rules obtained in Sec. III B we find the kneading sequence of a 2^5 cycle for the function $\tilde{u}$:

$$R\ RL\ RL\ LR\ RL\ LR\ LR\ RL\ RL\ LR\ LR\ RL\ LR\ RL\ RL\ LR\ C\ . \tag{4.7}$$

Dropping the first R we find that the shortest blocks are obtained by bunching pairs of symbols together to give RL and LR. For a cycle of length 2^n with $n\to\infty$, renaming $RL\to R$, $LR\to L$ gives an invariant kneading sequence. In terms of first-return maps this procedure yields the box shown in Fig. 6, as is explained in Sec. IV D. In contrast to the unimodal formulation there appears no second region J' for generating a RG scheme. In a similar way one can rephrase in terms of $\tilde{u}$ all the n-tuplings seen for one-hump maps.[14,15] In all these cases one can perform the usual functional RG. If one wants to have a single unstable eigenvalue one has to limit the functional perturbations to the subspace of codimension 1 of antisymmetric functions. More general perturbations give rise to two unstable eigenvalues.

D. Determination of the return interval

In contrast to one-hump maps one can determine the return interval associated with a given block renaming for maps in U as systematically as one did it for continuous circle maps. The ideas is to look at the two given blocks, say block B_L of m symbols and block B_R of n symbols. We know that the return map will contain two branches, being the mth and nth iterate of the map, respectively, restricted to appropriate subintervals. These two branches form a discontinuity which is the new $\tilde{x}_c$ for the return map. Thus the return interval is naturally subdivided into two subintervals separated by the point $\tilde{x}_c$. We can use this fact for finding $\tilde{x}_c$; realizing that the two subintervals correspond to points whose itineraries start with the symbols that appear in the blocks, the common point $\tilde{x}_c$ has to have an itinerary consisting of the common head of the blocks terminated by a C. Thus, for example, if $B_R=RRL$, $B_L=RL$, we look for the $\tilde{x}_c$ whose itinerary is RC. (We remark that in order to guarantee the uniqueness of $\tilde{x}_c$ one has to restrict the class of maps that we consider, for example, to the class of C^3 maps with negative Schwarzian derivative, i.e., $[(u'''/u')$

$-\frac{3}{2}(u''/u')^2]<0.$) Once $\tilde{x}_c$ has been found the boundaries of the return interval are determined as the left limit of the mth and the right limit of the nth iterate of the map as x goes to $\tilde{x}_c$.

E. New scenarios in U space

1. Preliminaries

To demonstrate the richness of dynamical behavior of maps in the space U we select a particular two-parameter family of the form

$$u_{\mu,\nu}(x)=\begin{cases}+\nu-x^2, & x\le 0\\ -\mu+x^2, & x>0\,,\end{cases} \tag{4.8}$$

from the interval $[-\mu,\nu]$ to itself. The parameters μ,ν are chosen such that

$$\begin{aligned}&-\mu+\nu^2\le\nu\,,\\ &\nu-\mu^2\ge-\mu\,,\end{aligned} \tag{4.9}$$

see Fig. 7. The condition $\mu=\nu$ corresponding to the first diagonal yields antisymmetric maps equivalent to unimodal ones, whereas the condition

$$\nu-\nu^2=\mu^2-\mu\,, \tag{4.10}$$

corresponding to the "second diagonal," yields continuous circle maps.

The notion of winding number introduced above continues to be useful for maps in this family, since left and right branches always exist. For values μ,ν below and on the line termed the second diagonal (see Fig. 8) the maps have a unique winding number. An easy way to see this fact is to recognize that for these values of μ,ν the maps can be considered as inverses of continuous circle maps with a flat part in their graph, see Fig. 9. Consequently, this region of the (μ,ν) plane is naturally partitioned into subregions which are characterized by their rotation numbers. This is similar to the partition of the (K,Ω) plane of the more familiar[16,17] sine-circle map $\theta'=\theta+\Omega-(K/2\pi)\sin(2\pi\theta)$, mod1, for values of $K\le 1$. Irrational winding numbers in this region are living on lines, again similarly to the sine-circle map. An advantage of the present family compared to sine-circle maps is the fact that maps in the family are always monotonically increasing so that kneading theory can be formulated with essentially two symbols. Consequently, it is easier to order the kneading sequences in the present case. One can show, for example, that the winding number (which can be read off the kneading sequence) is monotonically decreasing with μ, and monotonically increasing with ν.[18] Above the second diagonal one can lose the uniqueness of the winding number, but one can define a winding or rotation interval[19,20] $R(u_{\mu,\nu})$ comprising all w for which there is a $u_{\mu,\nu}$ orbit with rotation number w. Below the second diagonal the rotation interval contracts to a point, which is the winding number. The monotonic dependence of w on μ,ν below the second diagonal turns to a monotonic dependence of the boundaries of the rotation interval all over the (μ,ν) space.

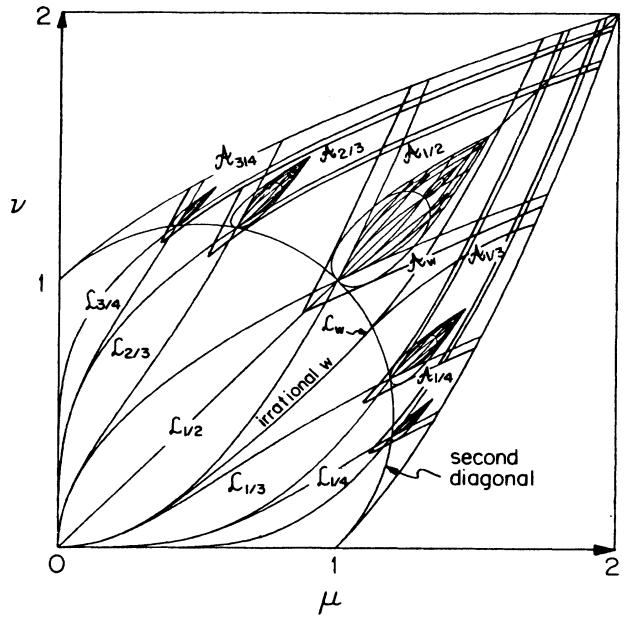

FIG. 8. Global structure of the phase diagram.

Essential questions are where is the borderline for chaotic behavior, and what is the dynamic behavior for

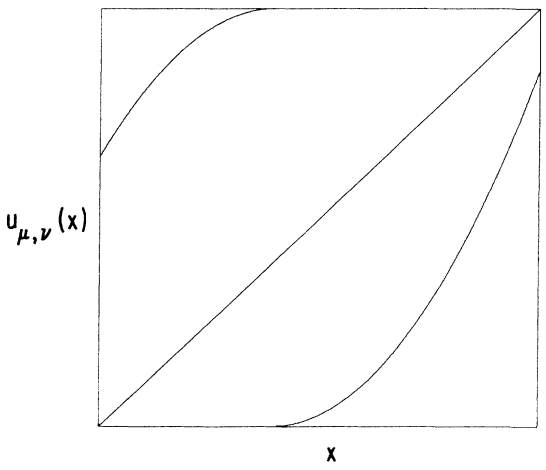

FIG. 7. Graph of a typical function $u_{\mu,\nu}$.

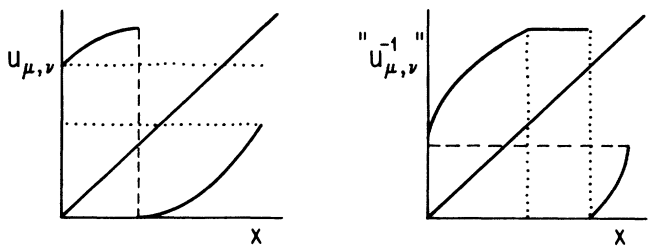

FIG. 9. $u_{\mu,\nu}$ below the second diagonal. The inverse function can be considered as a continuous circle map with a flat part in it.

maps on the borderline. In most physical applications, chaos is defined as the positivity of a Lyapunov exponent for "most" orbits (i.e., sensitivity to initial conditions).[21] A necessary condition for this "strong" chaos is the positivity of the topological entropy.[23] In our case this is equivalent to the existence of horseshoes.[22] For one-dimensional maps the map H has a horseshoe if there exists an interval A and two disjoint subintervals A_1, A_2 of A such that for some positive n both $h^n(A_1)$ and $h^n(A_2)$ cover A. An example of this situation is shown in Fig. 10(a) for some nth iterate of a map. We also show in Figs. 10(b) and 10(c) the relevant parts of the graphs of $(h^n)^2$ and $(h^n)^3$ where one sees that the number of intersections with the diagonal grows at least as 2^m for $(h^n)^m$. This means that there is an essentially exponential growth (in the sense of lim sup) of the number of orbits of increasing length. For maps in U whenever there is a nontrivial rotation interval the topological entropy is positive. The way to see this is to think about an interval whose two end points have two different rotation numbers. After a sufficient number of iterations the image of this interval will cover the whole circle many times.[23] In particular it covers it at least twice, and therefore we have a horseshoe.

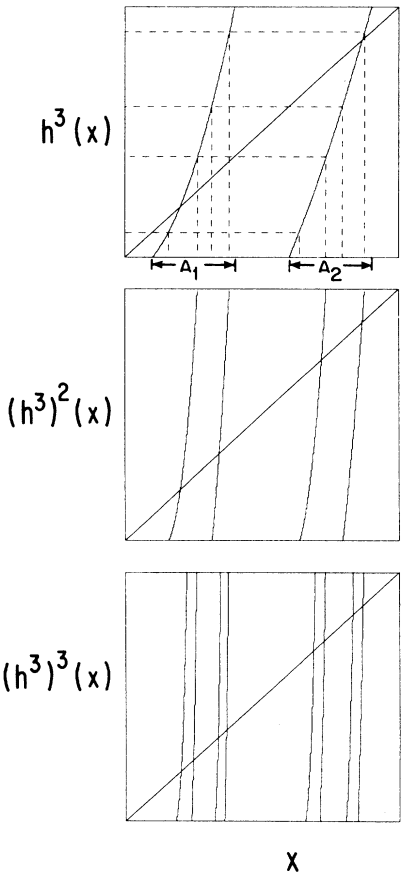

FIG. 10. Horseshoe in one-dimensional mappings. If h^n has at least two branches mapping A_1 and A_2 to the whole interval, the number of branches increases at least exponentially because the number of preimages of A_1 and A_2 is doubled with each iteration of h^n.

In analogy to continuous circle maps we define Arnold tongues and frequency-locked regions as the regions $\mathscr{A}_w$ such that $(\mu,\nu)\in\mathscr{A}_w$ if and only if $w\in R(u_{\mu,\nu})$ and $\mathscr{L}_w$ such that $(\mu,\nu)\in\mathscr{L}_w$ if and only if $R(u_{\mu,\nu})\equiv\{w\}$, respectively. A qualitative sketch of such regions is displayed in Fig. 8, where both regions are shown for rational and an irrational w.

Examining more closely the structure of locking we realize that the lines where the winding number is well defined and irrational terminate at the second diagonal, and one can always approach the intersection point from above via maps that have winding intervals.[24] Thus, all the intersections of the irrational lines with the second diagonal belong to the boundary of chaos. To gain further understanding of the boundary of chaos we have, however, to examine more closely the structure of rational Arnold tongues.

2. *Structure of rational Arnold tongues*

To describe the rational tongues, let us denote by $(K^-_{p/q},K^+_{p/q})$ the kneading sequences of the rotation by an angle p/q. One can show that the lines $K^-=K^-_{p/q}$ and $K^+=K^+_{p/q}$ in the (μ,ν) parameter space cross at a point on the second diagonal, forming a pair of opposite wedges [see Fig. 11(a)]. This region belongs to $\mathscr{A}_{p/q}$ but does not exhaust it. In fact, the upper wedge is surrounded by a line. This line corresponds to a saddle-node bifurcation, except at the tips where one has a (symmetry-breaking) pitchfork bifurcation. The number of available orbits with rotation number p/q and the right itineraries is shown in Fig. 11(a).

Another line inside $\mathscr{A}_{p/q}$ plays a fundamental role; it is the line $\mathscr{H}_{p/q}$ which separates $\mathscr{L}_{p/q}$ from the rest of $\mathscr{A}_{p/q}$ (i.e., crossing it leads to the establishment of a nontrivial rotation interval). Now, the two pieces of the boundary of $\mathscr{A}_{p/q}$ above the second diagonal and which bound also $\mathscr{L}_{p/q}$ belong to the boundary of chaos [see Fig. 11(b)].

At this stage we can already say that the line formed by such pieces for all p/q, all $\mathscr{H}_{p/q}$'s, and the irrational points on the second diagonal form a first approximation to the boundary of chaos. Above this line, the rotation interval is nowhere reduced to a single point.

To proceed, let us, for each p/q denote by $\mathscr{R}_{p/q}$ the curvilinear quadrilateral formed by $\mathscr{H}_{p/q}$ and the lines $K^-=K^-_{p/q}$, $K^+=K^+_{p/q}$. Then the two pieces of $\mathscr{H}_{p/q}$ which do not penetrate to $\mathscr{R}_{p/q}$ belong to the boundary of chaos. In $\mathscr{R}_{p/q}$, $(u_{\mu,\nu})^q$ restricted to a properly chosen subinterval yields a problem identical in form to the original problem. Therefore, there will be similar Arnold tongues, frequency-locked regions, first and second diagonals, etc. As a consequence, the global aspects of the boundary of chaos will repeat themselves on smaller scales in each frequency-locked region, in all secondary frequency-locked regions inside them, and so on *ad infinitum*.

As a consequence, the global features of the phase diagram, sketched in Fig. 8, repeat themselves in each $\mathscr{R}_{p/q}$, yielding inductively a hierarchical structure. At each level of this hierarchy going from $\mathscr{L}_w$ to the rest of $\mathscr{A}_w$

when w is irrational, or leaving $\mathscr{L}_{p/q}$ from the region which is neither in $\mathscr{M}_{p/q}$ nor in $\mathscr{R}_{p/q}$ is tantamount to a transition to chaos. Analogous transitions can also be found in continuous circle maps.[25]

There are, however, new codimension-2 scenarios[26] generated by following paths from $\mathscr{M}_{p/q}$ to $\mathscr{R}_{p/q}$ at each level of the hierarchy. Such a step is referred to as $M(p/q \to w)$ to indicate in which locking one enters at the next level of the hierarchy. The generic path of this kind will therefore be characterized by $M(p_1/q_1 \to p_2/q_2)M(p_2/q_2 \to p_3/q_3)M(p_3/q_3 \to p_4/q_4)\cdots$ corresponding to successive $q_2, q_3, q_4, \ldots$ -furcations. The simplest ones correspond to cases where p_n/q_n does not depend on n. These are the ones which will yield a fixed point under renormalization.

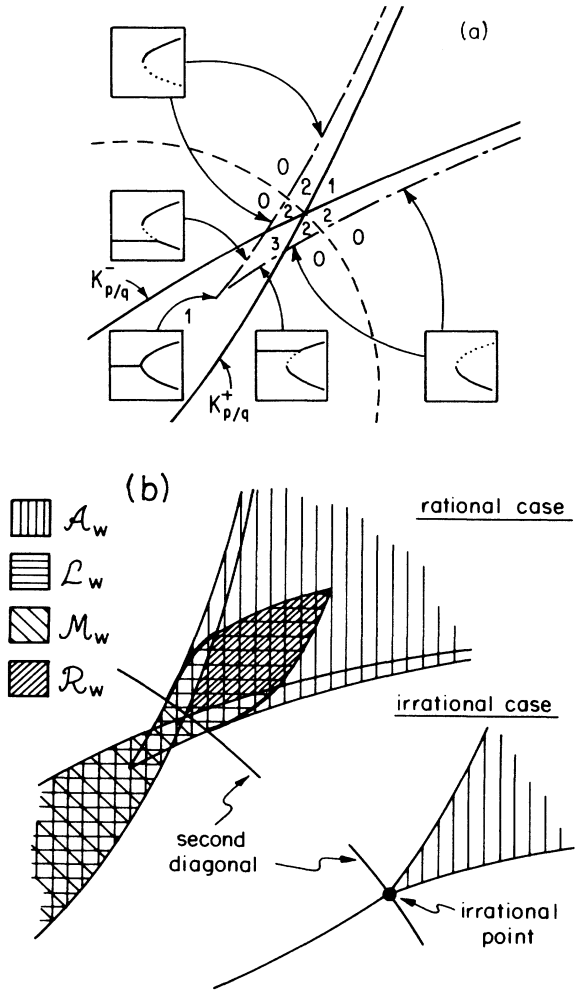

FIG. 11. (a) Structure of Arnold tongues near the second diagonal. The solid lines are defined by constant kneading sequences K^+ and K^- that terminate with a C. They intersect on the second diagonal (dashed). Above the inverted wedge (dotted) there is no mode locking. The saddle-node line (dash dotted) separates the two regions with trivial rotation intervals above and below the second diagonal. We have also indicated the number of distinct orbits with period q and rotation number p/q, with rotation-compatible itineraries. (b) $\mathscr{A}_w$ denotes the Arnold tongue, i.e., where there exists an orbit with winding number w. $\mathscr{L}_w$ denotes the region of frequency locking, i.e., all orbits have winding number w. $\mathscr{M}_w$ denotes the region of $\mathscr{A}_w$ below the second diagonal. $\mathscr{R}_w$ is the region where the q iterate of the map properly restricted belongs again to U. $\mathscr{H}_w$ separates $\mathscr{L}_w$ from the rest of $\mathscr{A}_w$.

F. Physical relevance of the space U: Connection to flows

It has been shown[13,27,28] that simple flows of the type of the Lorenz model,[29] which have a linearized form

$$\begin{aligned} \dot{x} &= \lambda_1 x \ , \\ \dot{y} &= -\lambda_3 y \ , \\ \dot{z} &= -\lambda_2 z \ , \end{aligned} \tag{4.11}$$

with $\lambda_2 < \lambda_3$, under Poincaré section may reduce to one-dimensional maps of the form $f:[-\mu,\nu] \to [-\mu,\nu]$,

$$f(x) = \begin{cases} +\nu - b\,|x|^{\zeta} + \text{higher-order terms}, & x < 0 \\ -\mu + a x^{\zeta} + \text{higher-order terms}, & x > 0 \ . \end{cases} \tag{4.12}$$

The exponent ζ is shown[29] to be

$$\zeta = \lambda_2/\lambda_1 \ . \tag{4.13}$$

All the arguments concerning the family (4.8) go over to these functions which belong to U, as long as $\zeta > 1$. (The case $\zeta < 1$ corresponds to the Lorenz model). We stress that ζ need not be an integer in general, and in particular ζ can be quite close to unity. The theory that we present next takes advantage of this fact. We examine now the scenario of trifurcations towards chaos. Clearly, any other scenario can be dealt with using similar methods.

It is worth noting that from the symbolic point of view the flows and the associated maps can be treated on the same footing. R and L for the flow simply mean loops of orbits on the rights and left sides, respectively, of the stable manifold of the origin.

G. Period tripling towards chaos

1. *Deriving the functional equations*

A first step in constructing a theory of period tripling is the derivation of the kneading sequences. We note that period tripling occurs a the point of intersection of the second diagonal with the homoclinic lines defined by $K = LRR$ and $K^+ = RRL$. Above the second diagonal we enter the tongue where the third iterate, restricted to an interval, again has winding number $\frac{2}{3}$ (i.e., we follow the path $M_{2/3}M_{2/3}M_{2/3}\cdots$). That tongue has homoclinic boundaries and the kneading sequences can be obtained as combinations of the kneading sequences of the order-3 cycles. These are $(RRL)^\infty$ and $(LRR)^\infty$. The condition that x_c belongs to the cycle changes them to RRC and LRC. The easiest way to obtain the kneading sequences of the order-9 cycles is to glue three order-3 cycles together. This procedure is clarified and generalized in Sec. VI. We pick the largest, e.g., RRL, increase it to RRR and

glue to it twice LRR, decreasing the last one to LRL. We obtain

$$(RRRLRRLRL)^{\infty} . \tag{4.14a}$$

This is K^+. K^- is obtained as the minimal permutation, i.e.,

$$(LRLRRRLRR)^{\infty} . \tag{4.14b}$$

The condition that x_c belongs to the cycle changes these to $RRRLRRLRC$ and $LRLRRRLRC$, respectively. The next pair of 27-cycles is obtained similarly,

$$\begin{aligned}&(RRR\ LRR\ LRR\ LRL\ RRR\ LRR\ LRL\ RRR\ LRL)^{\infty} \text{ for } K^+ ,\\ &(LRL\ RRR\ LRL\ RRR\ LRR\ LRR\ LRL\ RRR\ LRR)^{\infty} \text{ for } K^- .\end{aligned} \tag{4.15}$$

This process can be continued *an infinitum*.

Dropping the first R in K^+ we identify the blocks RRL, RLR, such that the blocking renaming

$$RRL \to R, \quad RLR \to L \tag{4.16}$$

leaves the asymptotic sequence invariant. Another block renaming is obtained by dropping the first two symbols and identifying the blocks RLR and LRR and rename

$$RLR \to R, \quad LRR \to L . \tag{4.17}$$

This leaves the sequence invariant as well.

These two block-renaming procedures are consistent with the two boxes of return intervals shown in Fig. 12. It is also straightforward to derive the functional equations defined by this RG. Denoting the right branch by u_R and the left branch by u_L we get for (4.17) [which is slightly more convenient than (4.16)] the functional equation of period tripling,

$$\begin{aligned}\tilde{u}_R(x)&=\alpha u_R \circ u_L \circ u_R(x/\alpha) ,\\ \tilde{u}_R(x)&=\alpha u_R \circ u_R \circ u_L(x/\alpha) .\end{aligned} \tag{4.18}$$

2. *Approximate solutions*

One can solve Eqs. (4.18) for the family (4.8). However, in view of the fact that natural reductions of flows lead to (4.12), with $\zeta \neq 2$ in general, we prefer to solve (4.18) approximately for the case $\zeta = 1+\epsilon$, with ϵ small.[14,28,30] The equations to be considered are therefore

$$\begin{aligned}-\tilde{\mu}+\tilde{a}x^{\zeta}&=\alpha(-\mu+a\{\nu-b[\mu-a(x/\alpha)^{\zeta}]^{\zeta}\}^{\zeta}) ,\\ \tilde{\nu}-\tilde{b}x^{\zeta}&=\alpha(-\mu+a\{-\mu+a[\nu-b(x/\alpha)^{\zeta}]^{\zeta}\}^{\zeta}) .\end{aligned} \tag{4.19}$$

The rescaling parameter α is found by noticing that the return box dictated by the block renaming (4.17) is bounded on the left by $-\mu+a(\nu-b\mu^{\zeta})^{\zeta}$. Since the left boundary of the original interval is at $-\mu$, we have

$$\alpha=\frac{-\mu}{-\mu+a(\nu-b\mu^{\zeta})^{\zeta}} . \tag{4.20}$$

Solutions for $\zeta=1$. When $\zeta=1$ we have

$$\alpha=\frac{-\mu}{-\mu+a(\nu-b\mu)} . \tag{4.21}$$

The functional equations (4.19) read in this case

$$\begin{aligned}-\tilde{\mu}+\tilde{a}x&=\alpha[-\mu+a(\nu-b\mu)+a^2b(x/\alpha)] ,\\ \tilde{\nu}-\tilde{b}x&=\alpha[-\mu+a(-\mu+a\nu)-a^2b(x/\alpha)] .\end{aligned} \tag{4.22}$$

The recursion relations are therefore

$$\begin{aligned}&\tilde{\mu}=\mu, \quad \tilde{a}=a_2b ,\\ &\tilde{\nu}=\frac{-\mu[-\mu+a(-\mu+a\nu)]}{-\mu+a(\nu-b\mu)}, \quad \tilde{b}=a^2b .\end{aligned} \tag{4.23}$$

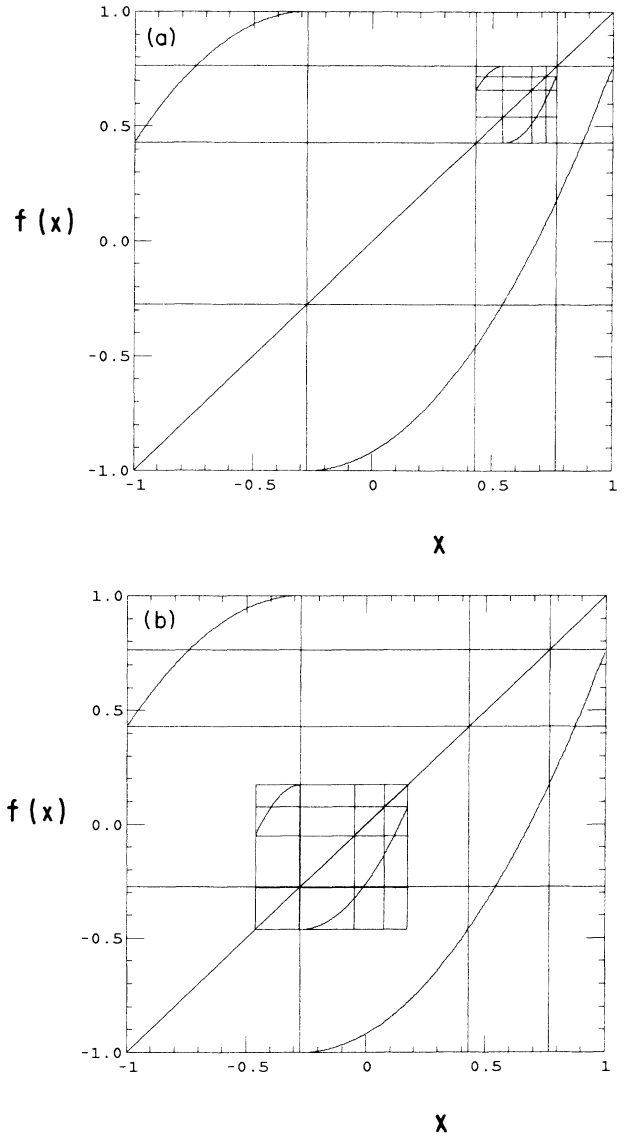

FIG. 12. Return maps for the block renaming rules. (a) $RLR \to L$, $RRL \to R$, (b) $LRR \to L$, $RLR \to R$.

We can conveniently take $\mu=1$, and find the fixed-point solution

$$a^*=b^*=1,\quad \nu^*=2,\quad \alpha=\infty\ . \tag{4.24}$$

Linearizing Eqs. (4.23) we find the three eigenvalues

$$\lambda_1=0,\quad \lambda_2=3,\quad \lambda_3=\infty\ . \tag{4.25}$$

Solution for $\zeta=1+\epsilon$. For $\zeta=1+\epsilon$ we are interested in the corrections to the relevant eigenvalues. We shall write

$$\nu=2+\eta,\quad b=1+\gamma \tag{4.26}$$

and we expect $\eta\to 0$, $\gamma\to 0$ when $\epsilon\to 0$.

It turns out that the freedom to choose $\mu=1$ continues in this case as well. We can thus write the rescaling ratio α as

$$\alpha=\frac{1}{1-a(\nu-b)^{1+\epsilon}}\ . \tag{4.27}$$

Using (4.26) and expanding to lowest order in ϵ we find

$$\alpha=-1/\eta\ . \tag{4.28}$$

The other recursion relations that we find upon expansion are

$$\tilde{\nu}=\alpha\frac{3\gamma+\eta+2\epsilon\ln 2}{-\eta},\quad \tilde{a}=(1+3\gamma)(-\eta)^{\epsilon}\ . \tag{4.29}$$

We write $\tilde{\nu}=2+\tilde{\eta}$, $\tilde{a}=1+\tilde{\gamma}$ we find the fixed-point equations

$$1+\gamma^*=(1+3\gamma^*)(-\eta^*)^{\epsilon}\ , \tag{4.30}$$

$$-\eta^*=\gamma^*+(2\epsilon\ln 2)/3\ . \tag{4.31}$$

Substituting Eq. (4.31) in (4.30) we find

$$(1+\gamma^*)/(1+3\gamma^*)=[\gamma^*+(2\epsilon\ln 2)/3]^{\epsilon}\ . \tag{4.32}$$

We write this as

$$1-2\gamma^*=\exp\{\epsilon\ln[\gamma^*+(2\epsilon\ln 2)/3]\} \tag{4.33}$$

or

$$(1+\gamma^*)^{-2/\epsilon}=\gamma^*=(2\epsilon\ln 2)/3=\exp(-2\gamma^*/\epsilon)\ . \tag{4.34}$$

Since for $\epsilon\to 0$ the left-hand side approaches 0, ϵ goes to zero faster than γ^*. Accordingly, Eq. (4.31) reads, to lowest order,

$$-\eta^*=\gamma^*\ . \tag{4.35}$$

To the same order Eq. (4.33) yields

$$\epsilon=\frac{\ln(1-2\gamma^*)}{\ln\gamma^*}=-\frac{2\gamma^*}{\ln\gamma^*}\ . \tag{4.36}$$

To get the eigenvalues around this fixed point we rewrite Eqs. (4.29) as

$$\tilde{a}=(3a-2)(2-\nu)^{\epsilon}\ , \tag{4.37}$$

$$\tilde{\nu}=\frac{3(a-1)+(\nu-2)}{(2-\nu)}\ . \tag{4.38}$$

Linearizing and solving the resulting matrix we find finally that the two relevant eigenvalues λ_2,λ_3 read now

$$\lambda_2=3-2/\ln\gamma^*\ , \tag{4.39}$$

$$\lambda_3=3/\gamma^*\ . \tag{4.40}$$

Using (4.36) we can evaluate these eigenvalues for given ϵ, as long as $\epsilon<\gamma$.

In Sec. V we compare numerical calculations to the predictions of this simple estimate of the eigenvalues. In the figures results of an ϵ expansion up to $O(\epsilon)$ are shown in addition to the lowest-order results reported here.

V. NUMERICAL RESULTS

We performed numerical computations to illustrate our theoretical results and to check the range of validity of the ϵ expansion in the RG calculation.

As an example for a discrete map we used

$$u_{\mu,\nu}=\begin{cases}+\nu-2x^{\zeta}, & x\le 0\\ -\mu+2x^{\zeta}, & x>0\ .\end{cases} \tag{5.1}$$

First, we computed the boundaries of the $p/q=2/3$ tongues and their intersection points (vertices) in the (μ,ν) phase diagram. We made use of the fact that each line is defined in terms of a kneading sequence $K^{\pm}$ and that these sequences are monotonic functions of μ and ν. The symbol C at the end of the respective sequence was realized by adjusting the parameters such that the corresponding iterate of $-\mu$ or ν was zero. Specifying a pair of block-renaming rules we generated a series of sequence pairs (K_n^-,K_n^+), $n=0,1,2,\ldots$. The intersections of the corresponding boundary lines yield a series of vertices (μ_n,ν_n), $n=0,1,2,\ldots$ accumulating at a point (μ_∞,ν_∞). Defining the length of the nth resonance tongue between the $(n-1)$th and nth vertex by

$$l_n=[(\mu_n-\mu_{n-1})^2+(\nu_n-\nu_{n-1})^2]^{1/2}\ , \tag{5.2}$$

we estimated

$$\delta_l=\lim_{n\to\infty}\frac{l_{n-1}-l_n}{l_n-l_{n+1}}\ . \tag{5.3}$$

δ_l may be thought of as describing "longitudinal" scaling properties in the phase diagram.

To obtain a corresponding number describing the "transversal" scaling we measured the breadths b_n of the resonance tongue $n=1,2,3\ldots$ and estimated

$$\delta_b=\lim_{n\to\infty}\frac{b_{n-1}-b_n}{b_n-b_{n+1}}\ . \tag{5.4}$$

The results are summarized in Table I, and Fig. 13(a). The value of α was computed from the ratios of the lengths of the intervals J in which the first return maps were restricted. In Fig. 13(b) we present the values of α from Table V, together with the results of the ϵ expansion of Sec. IV. Shown are both the lowest-order calculations presented above and the next-order calculations (i.e., up to terms linear in ϵ). From the numerical results of Table I it is tempting to conclude that the relevant eigenvalues λ_2 and λ_3 of Eqs. (4.39) and (4.40) are closely related to δ_l and δ_b, respectively.

TABLE I. Numerical results for $\delta_l, \delta_b, \alpha$.

ζ	δ_l	δ_b	α
1.02	3.90±2	123 ±4	39.8 ±0.5
1.05	4.16±0.11	66.4 ±41.2	20.5 ±0.1
1.10	4.52±0.07	43.4 ±0.5	12.82 ±0.04
1.20	5.10±0.01	29.95±0.04	8.195±0.003
1.30	5.62±0.01	24.94±0.01	6.394±0.003
1.40	6.11±0.01	22.34±0.01	5.401±0.005
1.50	6.61±0.03	20.82±0.01	4.765±0.007
1.60	7.11±0.06	19.92±0.05	4.32 ±0.03
1.70	7.64±0.11	19.46±0.15	4.00 ±0.05
1.80	8.29±0.21	19.38±0.38	3.78 ±0.10
1.90	8.95±0.45	18.89±0.6	3.68 ±0.24
2.00	9.91±1	18.34±0.6	3.28 ±0.5

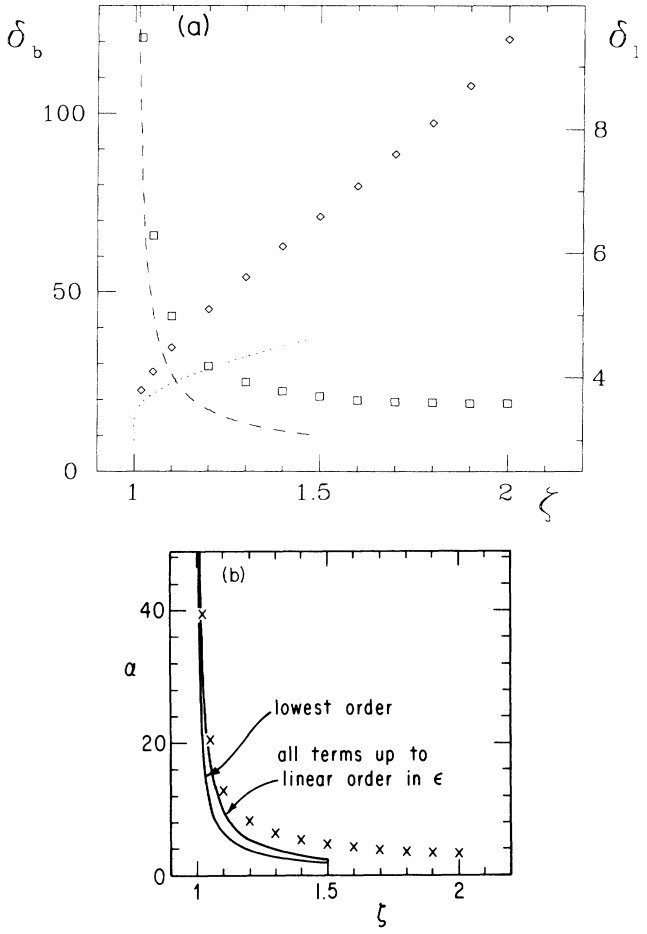

FIG. 13. (a) Results for δ_l and δ_b in the case of period tripling. The numerical values for δ_l (diamonds) and δ_b (squares) are obtained by extrapolation from the first five bifurcations along the period-tripling cascade defined by $RLR \to L$, $LRR \to R$. For $\zeta \to 1$ the numerical values approach those obtained by ϵ expansion around $\zeta = 1$. The dotted line represents λ_2 as given in (4.39) and the dashed one λ_3 according to (4.40). (b) Results for α in the case of period tripling. The numerical values are denoted with x. The lower curve is the result of ϵ expansion to lowest order, and the higher curve to order linear in ϵ.

VI. THE INFINITY OF SELF-SIMILAR STRUCTURES IN PARAMETER SPACE

Period tripling is but a particular example of the rich behavior seen while moving in parameter space. In this section we treat the general theory of q-tupling as well as mixed-tupling bifurcations, taking full advantage of the self-similarity of parameter space as discussed in Sec. IV. As has been advocated in this paper, we know how to build a theory, once we know the symbolic dynamics. In this context the crucial observation is that whenever a K^+ homoclinic sequence coexists with a K^- homoclinic one (i.e., at the points of intersection of homoclinic lines in parameter space) there ensues an infinite number of bifurcations. The simplest such point is $\mu = \nu = 0$ (see Fig. 8). Near this point (for positive μ and ν) all pairs of kneading sequences are of the form of a rotation and are naturally partitioned into blocks, as explained in Sec. III. Each such pair corresponds to one winding number.

To get the kneading sequences in vertices formed by the crossings of homoclinic lines in parameter space it is convenient to represent the dynamics near $\mu, \nu = 0$ as the itinerary of $x = x_c$ in addition to those of K^+ and K^-. To do that we simply use K^+ (homoclinic), and shift the C at the end to the beginning and make it an L. For the K^- we do the same but change C to R. (See examples below.)

To obtain kneading sequences at other vertices we pick any rotation number and consider the two corresponding itineraries of $x = x_c$ as constructed above. These itineraries are now used as a mold where each symbol is substituted by a group of symbols, according to K^+ and K^- of the vertex. The only additional trick is that these substitutions are made such that if the *following* symbol is R or L we finish the substitution with R or L, respectively. We give now a few examples to make the procedure clear.

Examples.

(i) 4/5 rotation number in the 2/3 vertex. The 2/3 vertex is the intersection of $K^+_{2/3} = RRC$ and $K^-_{2/3} = LRC$. The 4/5 rotation number is consistent with $K^+_{4/5} = RRRRC$ and $K^-_{4/5} = LRRRC$. The 4/5 itineraries of $x = x_c$ are therefore $LRRRR$ and $RLRRR$. Rewrite them as

$$(\tilde{L}\,\tilde{R}\,\tilde{R}\,\tilde{R}\,\tilde{R})^\infty, \quad (\tilde{R}\,\tilde{L}\,\tilde{R}\,\tilde{R}\,\tilde{R})^\infty . \tag{6.1}$$

Now perform the substitution

$$\tilde{L} \to RRC, \quad \tilde{R} \to LRC . \tag{6.2}$$

Substituting in Eq. (6.1) we follow the rule that if $\tilde{L}$ is followed by $\tilde{R}$, then $\tilde{L} = RRR$, whereas if $\tilde{R}$ is followed by $\tilde{L}$, then $\tilde{R} = LRL$. This gives the pair

$$\begin{aligned} &(RRR\ LRR\ LRR\ LRR\ LRL)^\infty , \\ &(LRL\ RRR\ LRR\ LRR\ LRR)^\infty . \end{aligned} \tag{6.3}$$

Notice that these sequences have winding number 2/3, but after block renaming they will be decimated to $K^+_{4/5}$ and $K^-_{4/5}$.

(ii) Period tripling with rotation number 2/3. The sequences RRC and LRC yield

$$(\tilde{L}\,\tilde{R}\,\tilde{R})^{\infty},\quad (\tilde{R}\,\tilde{L}\,\tilde{R})^{\infty}\ . \tag{6.4}$$

Substituting $\tilde{L}\rightarrow RRC$, $\tilde{R}\rightarrow LRC$ we get

$$\begin{aligned}&(RRR\ LRR\ LRL)^{\infty}\ ,\\ &(LRL\ RRR\ LRR)^{\infty}\ ,\end{aligned} \tag{6.5}$$

and compare Eq. (4.14).

Any other more or less esoteric combination can be treated with the same ease. One always get kneading sequences that have a natural block structure and are therefore amenable to the RG procedure that has been discussed in this paper. If one likes simple fixed points one has to simply iterate the process, starting with itineraries of x_c corresponding to the vertex one is looking at. With complicated RG's one can study many different scenarios for the onset of chaos, but this generally requires a lot of hard work.

As a final remark we note, that all examples of n-tuplings ($n\neq 2$) which were discussed before for maps of the interval correspond to the vertices on the first diagonal in (μ,ν) space. Additional points in (μ,ν) space away from the boundary of chaos in which there exist self-similar kneading sequences can be found. These points are treated with the help of the global theory built in Sec. VII.

VII. GLOBAL THEORY OF RENORMALIZATION GROUPS IN U SPACE

In Sec. VI we observed that given a scenario, we were able to construct the symbolic dynamics of the relevant orbits. Identifying the blocks in such sequences yielded a renormalization group, as has been demonstrated throughout this paper. In this section we show that symbolic manipulations allow us to get complete understanding of the types of RG's which exist and where to look for them in parameter space. We also describe briefly, using RG ideas, the fate of orbits whose itinerary does have a good block structure but where at least one of the kneading sequences (of the map) does not have the same block structure. In these cases the map is not renormalizable but in some sense the orbit is.

In the process we shall use the itineraries of x_c instead of the kneading sequences themselves. [We remember, however, that the kneading sequences can always be obtained from $I(x_c^-)=(LA)^{\infty}$ or $I(x_c^+)=(RB)^{\infty}$ simply as $K^+=(AL)^{\infty}$ and $K^-=(BR)^{\infty}$.] The reason for this change is that we want to discuss symbolic sequences in some generality; we do not follow a prescribed scenario as we did in the previous sections. It turns out that for this general discussion it is more natural to consider the above itineraries as will become clear in the sequel. Also, the main reasons for using kneading sequences before, i.e., their monotonicity in U space and their traditional use in dynamical system theory would not be crucial for the following discussion.

To derive itineraries of x_c we shall employ "inflation" rules which are also common in current theories of 1D quasicrystals. By an inflation rule we simply mean the "inverse" renaming rule,

$$\begin{aligned}&R\rightarrow W_1\ ,\\ &L\rightarrow W_2\ ,\end{aligned} \tag{7.1}$$

where W_1 and W_2 are blocks of R's and L's. In this language the previously defined block renamings can be thought of as "deflation" rules.

By "inflation process" we mean performing an infinite sequence of inflations. For instance, iterating (7.1) is a special inflation process in which a pair of sequences is generated. If one uses a "good" inflation rule this pair corresponds asymptotically to the two addresses of x_c. For concreteness we shall consider only order-preserving inflation rules. Thus all rules will be of the form

$$\begin{aligned}&L\rightarrow LA\ ,\\ &R\rightarrow RB\ .\end{aligned} \tag{7.2}$$

An obvious necessary condition is that A and B are such that $A(LA)^{\infty}$ is the upper bound on all its shifts and $B(RB)^{\infty}$ is the lower bound on all its shifts. Later we shall see that these conditions are not sufficient.

As examples we rederive some sequences that were obtained in previous sections.

(i) *Period doubling.* The rule is

$$\begin{aligned}&L\rightarrow LR\ ,\\ &R\rightarrow RL\ .\end{aligned} \tag{7.3}$$

The inflation process is

$$\begin{bmatrix}L\\R\end{bmatrix}\rightarrow\begin{bmatrix}LR\\RL\end{bmatrix}\rightarrow\begin{bmatrix}LRRL\\RLRR\end{bmatrix}\rightarrow\begin{bmatrix}LRRRLRLLR\\RLLRLRRL\end{bmatrix}, \tag{7.4}$$

etc., and compare Eq. (4.7).

(ii) *Golden mean rotation.* The inflation rule is

$$\begin{aligned}&L\rightarrow LR\ ,\\ &R\rightarrow RLR\ .\end{aligned} \tag{7.5}$$

The inflation process is

$$\begin{bmatrix}L\\R\end{bmatrix}\rightarrow\begin{bmatrix}LR\\RLR\end{bmatrix}\rightarrow\begin{bmatrix}LRRLR\\RLRLRRLR\end{bmatrix}\rightarrow\begin{bmatrix}LRRLRRLRLRRLR\\RLRLRRLRLRRLRRLRLRRLR\end{bmatrix}, \tag{7.6}$$

etc., cf. Eq. (3.13).

(ii) *4/5 rotation in the 2/3 vertex.* Combining

$$4/5\begin{cases}L\rightarrow LRRRR\\R\rightarrow RLRRR\end{cases}\text{ and }\ 2/3\begin{cases}L\rightarrow LRR\\R\rightarrow RLR\end{cases} \tag{7.7}$$

the inflation goes

$$\begin{bmatrix}L\\R\end{bmatrix}\rightarrow\begin{bmatrix}LRRRR\\RLRRR\end{bmatrix}\rightarrow\begin{bmatrix}LRRRLRRLRRLRRLR\\RLRLRRRLRRLRRLR\end{bmatrix} \tag{7.8}$$

and cf. Eq. (6.3).

The power of this approach can be demonstrated now by inverting the process. We can choose an inflation rule (or a set of them), and examine the significance of the pair of sequences obtained by iterating the inflation starting from the seed $\binom{L}{R}$.

(iv) *Example.* We have

$$\begin{aligned} &L \to LRR\ , \\ &R \to RL\ , \end{aligned} \tag{7.9}$$

$$\begin{bmatrix} L \\ R \end{bmatrix} \to \begin{bmatrix} LRR \\ RL \end{bmatrix} \to \begin{bmatrix} LRRRLRL \\ RLLRR \end{bmatrix} \to \begin{bmatrix} LRRRLRLRLLRRRLLRR \\ RLLRRLRRRLRL \end{bmatrix}, \tag{7.10}$$

etc.

A common feature of examples (i) and (iv) [and also of the single step of (iii)] is that at each step of the inflation the pair obtained corresponds to an actual itinerary of x_c of a map in U space. The way to see this is to realize that in these examples $A(LA)^\infty$ and $B(RB)^\infty$ are the upper and lower bounds, respectively, on all the shifts obtained on these two words. From general results about kneading sequences in U space one can show that this is a sufficient condition for the pair of sequences to correspond at each step to itineraries of x_c of some actual map in U.

This property is by no means trivial, and is certainly not satisfied by an arbitrary pair (A,B). Furthermore, it is not even a necessary condition for building up asymptotically a pair of itineraries of an actual map. For instance, see example (ii). In this case one has at each finite step itineraries of two different maps, corresponding to different winding numbers. Since these winding numbers are Farey neighbors, and they converge eventually to the golden mean, asymptotically one has the two itineraries of x_c for a map in U.

In fact, we conjecture that in general either one of the two following conditions should be met by a proper inflation in order to generate asymptotically nontrivial[31] itineraries of an actual map.

(i) $A(LA)^\infty$ and $B(RB)^\infty$ are maximal and minimal, respectively.

(ii) $(LA)^\infty$ and $(RB)^\infty$ are, respectively, K^- and K^+ for two rotations whose winding numbers are Farey neighbors. Consequently inflation rules of this type should be continued *ad infinitum*.

Notice that one can obtain proper inflations by first iterating type (ii) *ad infinitum* and then inflating the result according to rules of type (i). For instance, inflating the golden-mean pair (7.6) according to the period-doubling rule (7.3) leads to the pair

$$\begin{aligned} &LRRLRLLRRLRLLRRL\ldots\ , \\ &RLLRRLLRRRLRLLRL\ldots\ . \end{aligned} \tag{7.11}$$

This pair corresponds to the golden-mean line which lives below the *secondary* second diagonal inside the 1/2 frequency-locking region.

Notice that one can inflate using a different rule at each step. All proper asymptotic itineraries are produced by using infinitely many steps of type (i), or infinitely many steps of type (ii), or a finite number of steps of type (i) starting from an asymptotic state of type (ii).

This finishes the symbolic part of the discussion and we can turn now to questions of renormalization. For simplicity we focus on symbolic sequences obtained by iterating a single inflation rule and which have therefore a fixed point under block renaming. The rest of the discussion will be essentially conjectural; proving some of the statements involves difficult issues concerning, e.g., functional equations, etc.

We shall refer to fixed points of type (i) [(ii)] as those fixed points associated with itineraries obtained by inflations of type (i) [(ii)]. In a typical two-parameter family in U space, fixed points of type (i) live at the tips of vertices whose edges are defined by constant kneading sequences, which are K^+ and K^- of the tip. These tips are accumulation points of series of tips of similar vertices, corresponding to pairs of itineraries obtained by a finite number of inflation steps. Near such accumulation points we expect usual geometric scalings in parameter space as well as geometric scaling of the orbits at the tip. An inverse cascade will appear at reversed vertices (cf. Fig. 8). As usual (i.e., like in period doubling), scaling of the topological entropy is given by the same exponents as for the direct cascade.

In the rest of the vertex one can find trajectories which have an itinerary like *one* of kneading sequences at the tip. However, their scaling properties are quite different. Rather than having closest return which scale exponentially, their closest returns scale as exponentials of exponentials. Similarly, we can consider a path in parameter space that ends at a point on one of the edges of an asymptotic vertex. If this line cuts transversely through the corresponding edges of the approximating vertices, the points of cuts will converge again by an exp(exp) scaling law. The reason for these "superfast" convergences will be given shortly.

Fixed points of type (ii) will live on the fundamental second diagonal at the points where it is cut by quadratic irrational lines. These points are simultaneously tips of vertices in the chaotic regime and ends of lines in the subcritical regime. [See Fig. 11(b).] The discussion of the tip and its vertex follow precisely the analysis of type (i). The irrational "tails" call for further analysis.

The situation on subcritical irrational lines that terminate on the second diagonal is interesting; the orbits observed have the same ordering as usual rotations, but they do not fill up the interval. In fact, their closures are stable Cantor sets. This phenomenon is interesting as an example of stable Cantor sets far from the chaotic regime. We point out that such orbits were never observed (to our knowledge) in dynamical experiments, and it appears worthwhile to look for them in flows of the type considered in Sec. IV.

From the point of view of scaling behavior we expect that these orbits will again show superfast [exp(exp)] convergences in phase space. In addition, rational approximants corresponding to finite inflations will again converge in a superfast fashion.

The reason for all those superfast scaling behaviors is the following: although the orbits have good symbolic itineraries that are invariant under block renaming, the associated maps are not globally renormalizable. This is the case both in the subcritical and in the chaotic regimes.

In the subcritical region there is a gap in the image of the function. Therefore the inverse map has flat parts. (See Fig. 9.) Consequently, the inverse map belongs to the

stable manifold of a degenerate fixed point of the renormalization group, which is flat everywhere. (The same conclusion is reached by considering the map itself, but this way of looking at the problem unifies the superfast behavior on both sides of the second diagonal.)

In the chaotic regime one is led to maps with flat parts as well, but it is less straightforward to see this. Consider as an example the trajectory whose itinerary is the K^+ of the golden-mean rotation, for a map which lives on the first diagonal, see Fig. 14. There are two interesting possibilities: (i) The map lives on the edge of the vertex (the point B), or (ii) the map belongs anywhere on the first diagonal inside the vertex. In case (i) K^+ of the map is the same as K^+ of the golden mean. Denoting the map by $u(x)$, we note then that the orbit never visits points lower then $u(1)$ on the left branch. This is clear since K^+ comes from a rotation, and the sequence obtained by deleting the first symbol of K^+ is the lower bound for all sequences obtained by shifting up to any L. Accordingly, the map can be cut as in Fig. 15, yielding the map (b). This map is a continuous circle map with a flat part. For an analysis of the superfast behavior in such cases, see Sec. 4.4 of Ref. 32. Note that this analysis is done specifically for the golden-mean rotation number, and without a fixed-point theory. Combining this, however, with known results concerning RG for trapezoidal maps in the period-doubling case, we are led to the conjecture that superfast behavior would be the rule for any RG scheme whenever flat parts instead of critical points appear in the map. One expects having a degenerate fixed point which leads to superfast behavior in phase space and which possesses an infinite eigenvalue which dictates superfast convergence in parameter space.

If we are inside the vertex the situation is that of Fig. (16), with a point x_0 chosen such that $I(x_0)=K^+_{W_G}$. One can see that the orbit is restricted to the box shown. An analysis of maps of this kind, having no critical points, has been presented for the golden-mean case in Sec. 4.3 of Ref. 32. Notice that the fine details of the superfast convergence are nonuniversal and depend on whether or not

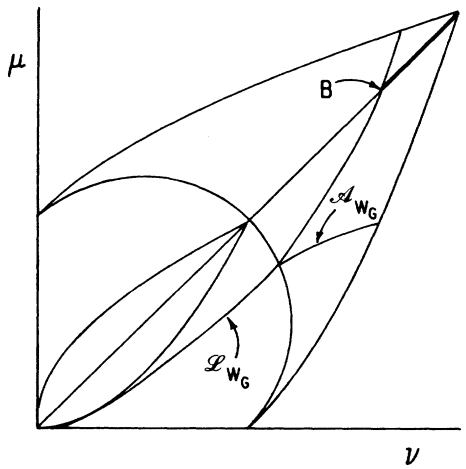

FIG. 14. The crossing of the line of fixed $K^+_{w_G}$ with the first diagonal. See text for explanation.

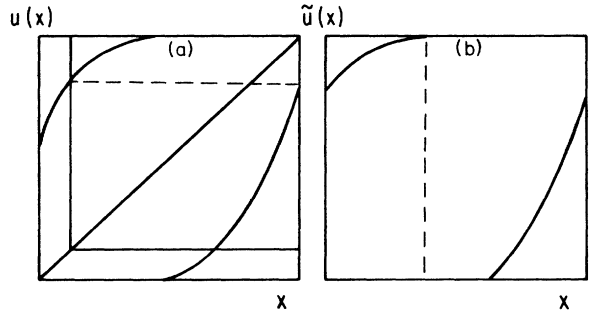

FIG. 15. Typical map at the point B of Fig. 14, and (b) the reduction to a map with a flat part.

there is a critical point. The phenomenon itself appears, however, to be superuniversal. It is also quite relevant because it is a *stable* phenomenon and can be found in an open region of parameter space. Obviously identical behavior exists in unimodal maps because of the equivalence discussed in Sec. III. It has also been observed in cubic continuous maps of the interval. Even more importantly such behavior will persist if one perturbs such 1D maps to diffeomorphisms of the plane, which are cross sections of physical flows.

VIII. SUMMARY AND DISCUSSION

The basic idea of this paper is that first-return maps together with topology are the crucial aspects underlying renormalization. In all renormalizable cases, understanding the topology via symbolic dynamics facilitates enormously the construction of a renormalization group. From this work it appears that "good" symbolic dynamics is essential for turning the unifying idea of first-return map, which was introduced here, into an operative procedure. We note that the idea of using first-return maps to capture the universal aspect of the dynamics is implicit already in Poincaré's use of such maps; defined for flows the first-return map eliminates the shape of the trajectory which is *a priori* irrelevant for topological and metric universality.

In the context of 1D maps we were able to go beyond the conceptual unification by introducing a space of functions that contained as particular cases all previously

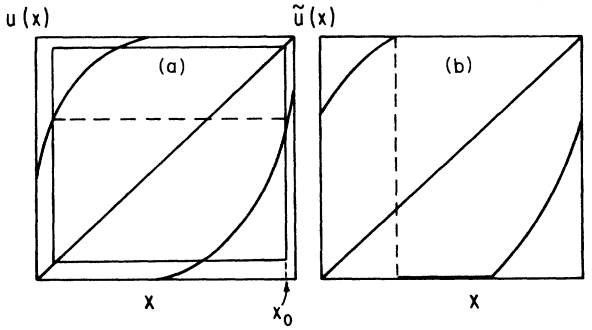

FIG. 16. The same as Fig. 15, for a typical map whose parameters are as those on the heavy segment of the first diagonal in Fig. 14.

known scenarios for the transition to chaos. This space displayed uncountably many new scenarios. All old and new scenarios which enjoy self-similarity can be treated in a unified fashion as shown above.

The issue of renormalization off the borderline of chaos was treated making full use of the symbolic dynamics. One of the conclusions is that there exists superuniversality in the superfast character of the convergence of orbits with good symbolic properties, as well as in the convergence in parameter space except at special points where both kneading sequences admit the same block structures. The final comment is that it appears that a proper renormalization-group theory should encompass all the available universal behaviors so that one would not have to solve infinitely many independent functional equations one by one.

We finish this paper with some bibliographical references. It seems that the first time that the symbolic sequence (7.4) appeared was in 1851, in the work of Prouhet in the context of arithmetics.[33] Systematic studies of such sequences started with the work of Thue[34] at the turn of the century. The first recognition of their roles in dynamics appears to go back to Morse in 1921.[35] Since then they became quite important in ergodic theory as well as in other branches of mathematics. Further references can be found in Ref. 36. Inflation rules can also be considered as automata and the role of such automate in the renormalization of unimodal maps has been recognized.

ACKNOWLEDGMENTS

This work has been supported in part by the Israel Academy of Science, the Comission for Basic Research, and by the Minerva Foundation, München, Germany. We acknowledge useful discussions with J. M. Gambaudo. The history of substitution rules has been recognized in Ref. 37.

---

*Permanent address: Institut für Festkörperforschung der Kernforschungsanlage, D-5170 Jülich, W. Germany.

†Also at the Hebrew University of Jerusalem and at the Mathematics Department of the Weizmann Institute of Science, Rehovot, Israel. Permanent address: Physique Theorique, Parc Valrose 06034 Nice Cedex, France.

[1]For a collection of relevant papers see *Chaos,* edited by Hao Bai-Lin (World Scientific, Singapore, 1984).

[2]M. J. Feigenbaum, J. Stat. Phys. **19**, 25 (1978); **21**, 669 (1979).

[3]P. Coullet and C. Tresser, J. Phys. (Paris) Colloq. **C5**, 25 (1978); C. R. Acad. Sci. Paris, Ser. A **287**, 577 (1978).

[4]M. J. Feigenbaum, L. P. Kadanoff, and S. J. Shenker, Physica **5D**, 370 (1982).

[5]D. Rand, S. Ostlund, J. Sethna, and E. D. Siggia, Physica **8D**, 303 (1983).

[6]For a different attempt of unification see H. Epstein (unpublished).

[7]For all issues concerning kneading sequences of one-hump maps see P. Collet and J.-P. Eckmann, *Iterated Maps on the Interval as Dynamical Systems* (Birkhäuser, Boston, 1980), and references therein.

[8]L. P. Kadanoff, Physica **2**, 263 (1966).

[9]H. Poincaré, J. Math. Pure Appl. **1**, 167 (1885) [in *Oevres Completes* (Gauthier Villars, Paris 1951), Vol. 1].

[10]J.-M. Gambaudo, O. Lanford, III, and C. Tresser, C. R. Acad. Sci. Paris, Ser. I **299**, 823 (1984).

[11]M. J. Feigenbaum and B. Haslacher, Phys. Rev. Lett. **49**, 605 (1982).

[12]O. E. Lanford, Bull. Am. Math. Soc. **6**, 427 (1982).

[13]A. Arneodo, P. Coullet, and C. Treser, Phys. Lett. **81A**, 197 (1981).

[14]B. Derrida, A. Gervois, and Y. Pomeau, J. Phys. A **12**, 269 (1979).

[15]S.-J. Chang and J. McCown, Phys. Rev. A **31**, 3791 (1985).

[16]V. I. Arnold, AMS Transl. **46**, 213 (1965).

[17]M. H. Jensen, P. Bak, and T. Bohr, Phys. Rev. A **30**, 1960 (1984).

[18]C. Tresser, C. R. Acad. Sci. Paris, Ser. I **296**, 729 (1983).

[19]S. Newhouse, J. Palis, and F. Takens, Pub. Math. I.H.E.S. **57**, 5 (1983).

[20]J.-M. Gambaudo and C. Tresser, C. R. Acad. Sci. Paris, Ser. I, **300**, 311 (1985); J.-M. Gambaudo and C. Tresser (unpublished).

[21]D. Ruelle, Ann. N.Y. Acad. Sci. **316**, 408 (1979).

[22]R. Bowen, *On Axiom A Diffeomorphisms,* Vol. 35 of *CBMS Regional Conference Series in Mathematics* (AMS, Providence, 1978).

[23]Notice that this argument which is trivially true for continuous circle maps is less straightforward for discontinuous maps. In the cases considered here it holds true because above the second diagonal the interval is not split by the discontinuity.

[24]To be more precise, this statement is true only for sufficiently smooth maps, see. e.g., Ref. 19.

[25]For a review of transitions to chaos in circle map see R. S. McKay and C. Tresser, Physica **19D**, 206 (1986).

[26]P. Collet, P. Coullet, and C. Tresser, J. Phys. Lett. (Paris) **46**, L146 (1986).

[27]J. Guckenheimer, Appl. Math. Sci. **19**, p. 368 (1976).

[28]J.-M. Gambaudo, I. Procaccia, S. Thomae, and C. Tresser, Phys. Rev. Lett. **57**, 925 (1986).

[29]E. N. Lorenz, J. Atmos. Sci. **20**, 130 (1963).

[30]P. Collet, J.-P. Eckmann, and O. E. Lanford, Commun. Math. Phys. **76**, 211 (1980).

[31]By nontrivial we mean nonperiodic.

[32]L. P. Kadanoff, J. Stat. Phys. **31**, 1 (1983).

[33]E. Prouhet, C.R. Acad. Sci. **33**, 225 (1851).

[34]A. Thue, K. Nor. Vid. Selesk. Skr. **7**, 1 (1906).

[35]M. Morse, Trans. Am. Math. Soc. **22**, 84 (1921).

[36]F. M. Dekking, Thesis, University of Nijmegen, 1980.

[37]J. P. Allonche and M. Cosnard, C. R. Acad. Sci. Paris, Ser. I **296**, 159 (1983).